

STUDY OF THE ELECTROCHEMICAL BEHAVIOUR OF A CARBON STEEL IN A REAL AND TREATED GEOTHERMAL ENVIRONMENT

Mohamed Amalhay, Catherine Cotiche and Ioannis Ignatiadis

BRGM, Research Division, Department of Geotechnical Engineering and Mineral Technology,
Avenue de Concy, BP 6009, 45060 ORLEANS, (France).

Key words: carbon steel, corrosion, inhibitor, geothermal environment, hydrogen sulfide, electrochemical techniques

ABSTRACT

The geothermal installations exploiting the Dogger aquifer in the Paris Basin encounter operational difficulties in the form of corrosion of carbon steel well casings, scaling and clogging, due essentially to the corrosivity of the fluids. In order to optimize anticorrosion treatment in geothermal wells, various corrosion inhibitors were tested on site. Using electrochemical techniques (monitoring of open circuit potential as a function of time, measurement of corrosion rates from Tafel plots, polarisation resistance and electrochemical impedance), different corrosion inhibitors were selected, characterized and compared according to their efficiency in reducing the carbon steel corrosion rate in a real geothermal environment.

1. INTRODUCTION

French "low enthalpy" geothermal energy is primarily used for the heating of housing units and the production of hot water. The water of the Dogger aquifer, exploited at the present time by around 40 geothermal doublets in the Paris region is highly mineralized and contains dissolved gases, including hydrogen sulfide (H_2S) and carbon dioxide (CO_2). The main physico-chemical characteristics of the fluids are temperatures ranging from 47 to 85 °C, pH between 6.1 and 6.5, total dissolved salts (TDS) between 6 and 35 g/l, of which is Cl^- , $[H_2S, HS^-]$ from 5 to 100 mg/l, $[SO_4^{2-}]$ from 300 to 1200 mg/l, $[CO_2/HCO_3^-]$ from 250 to 600 mg/l and no oxygen under normal conditions. These characteristics make it one of the most corrosive natural fluids for carbon steel (Ellis, 1981).

Some authors have shown that at such high concentrations the H_2S forms non-protective deposits (Ikeda *et al.*, 1985) and activates corrosion of carbon steel. Actually, their action is such that it increases the number of active dissolution centres and activates the reduction process by favouring the discharge of hydrogen (Pound *et al.*, 1980 and 1985). High concentrations of CO_2 in the geothermal environment buffer the medium and participate actively to the corrosion. Indeed, at the temperature and pH of the fluid, the CO_2 , mainly in dissolved form, produces very soluble corrosion products such as iron hydrogenocarbonate $Fe(HCO_3)_2$, and less soluble and more protecting products such as iron carbonate $FeCO_3$. Nevertheless, since the distribution of the latter is not homogeneous, pitting has been observed in sites near iron carbonate (Ikeda *et al.*, 1985; Crolet, 1988). Moreover, Cl^- increase the risk of corrosion by pitting and favour the dissolution of protective layers. Various theories and mechanisms have been suggested to explain the effect of these ions on the protective layers of the substrates (Lin *et al.*, 1981 and 1984; Pou *et al.*, 1984; Sato, 1982; Pickering and Frankenthal, 1972). The analysis of polished sections by X-ray images (EDS) of the scale from various depths in geothermal wells shows that the chloride ion content in these deposits increases as we move from the scale-solution interface towards the scale-metal interface (Amalhay *et al.*, 1994a). This confirms the preponderant role of Cl^- in the activation of corrosion. These deposits have two distinct layers. The first, inside, layer is formed essentially of iron salts such as $FeO(OH, Cl)$, $(FeCl_2, 4H_2O)$, $Fe_2(OH)_3Cl$, of iron carbonate ($FeCO_3$) and of iron sulfide (Fe_xS_y) in small quantities. The second, outside, layer is made up predominantly (80%) of iron sulfide (Amalhay *et al.*, 1994a). This iron sulfide is for the most part made up of mackinawite. The other phases of iron sulfide such as pyrite,

marcasite, greigite and pyrrhotite are all present but in small proportions. The scale, because of the fact that its standard potential is greater than that of metal, can even contribute to an increase in corrosion kinetics. Some authors (e.g., Rhodes, 1976) have shown that iron sulfides are cathodic sites facilitating the discharge of hydrogen as indicated above.

In order to improve operating conditions of geothermal exploitation in the Paris region, most of the doublets have been treated by corrosion inhibitor since 1989. Most of the corrosion inhibitors currently being used for the treatment of wells are quaternary ammonium salts which have proved their effectiveness in the field of petroleum. The objective of this study is to compare the effectiveness of these products and other molecules or formulas not yet on the market and to better understand the mechanisms controlling the inhibition of corrosion of carbon steel in geothermal fluids. We also attempt to determine the optimal concentration of inhibitor. It must be sufficiently effective at economically feasible concentrations and there must be no risk under certain conditions of favouring localised corrosion. Finally, it would be of interest to evaluate the adsorption-desorption kinetics of inhibitors in order to determine how long the inhibitor remains effective after treatment has ceased.

2. MATERIALS AND METHODS

The study consists in determining, by electrochemical measurements, the corrosion rate of a carbon steel identical to that of casings in a real geothermal environment as a function of immersion time and tensioactive compound concentration. The on site experiments have the advantage of using an aqueous medium which it is almost impossible to duplicate in the laboratory. Corrosimetric experiments were done on stationary and rotating samples in static reactors of a small volume so that initial conditions could be easily reproduced for short experimental times. The temperature in the cells was 65 °C. The pH was that of real geothermal fluid, 6.4. Six organic inhibitors were tested at concentrations of 0, 2.5 and 5 mg/l. The products tested are:

- Solamine 129R, Norus 491, Aquaprox MIX' 1300, formulations of surfactants already used for the treatment of geothermal wells or for combating boiler scaling (Aquaprox)
- Fatty Amine, Soluble Amine, Cyclic Amine are synthetic industrial molecules or formulations of surfactants the nature of which are industrial secrets. These are not yet commercialised and are still the object of research concerning their effectiveness in inhibiting corrosion and crystal growth.

The geothermal fluid was collected at the production wellhead and sent through insulated pipes to measurement cells upstream from which a flowrate regulator enabled us to maintain a flowrate of 30 l/h. The inhibitor was injected directly into the two electrochemical cells (one containing a stationary sample, the other a rotating sample) by means of two electric pumps of the HPLC type.

The measurement of corrosion rate and the assessment of the inhibitive action of the formulas tested were done with stationary and transitory electrochemical methods.

The electrochemical behaviour of the material (API K55 type carbon steel) in the geothermal medium was studied with linear potential sweep voltammetry. The plotting of cathodic and anodic polarisation curves is done in the potentiodynamic mode with a sweep rate of 0.1 mV s^{-1} in order to ensure quasi-stationary conditions. To measure polarisation resistance, the sweep covers only 20 mV around the open circuit corrosion potential, usually at the same sweep rate and in the same direction.

Before each polarisation test, the open circuit potential (E_{corr}) was monitored. It enables us to detect whether the surface becomes noble by the formation of passive films and helps us to determine stationary conditions, needed before any electrochemical measuring can be done. The determination of the polarisation resistance, R_p , equal to the reciprocal of the slope of the current vs. potential at the vicinity of the E_{corr} , gives the corrosion rate. This technique is based on the same theoretical hypotheses as the Tafel law but the fact that it applies to low overpotentials, anodic and cathodic, enabled Stern and Geary (1957) to simplify its mathematical formalism and to linearly link the current taken by the metal to the potential imposed and, consequently, to link R_p to the corrosion current (I_{corr}) according to the following equation.

$$I_{\text{corr}} = \frac{1}{2.303(b_a + b_c)R_p}$$

where b_a and b_c are the anodic and cathodic Tafel slopes, respectively.

The application of the Tafel law assumes a pure transfer regime that will be shown below. Knowing the density of the corrosion current, the corrosion rate is determined using the Faraday's formula. The effectiveness of the inhibitor is determined using the values of corrosion rate in the presence and absence of inhibitor.

We therefore used non-stationary electrochemical methods based on the analysis of the response of the metal-solution interface during the application of an external disruption of low amplitude. Electrochemical impedance measurements were carried out in the frequency range of 10^5 to 10^{-3} Hz. The measurement was done in the open circuit of steel with a disruption of 5 mV peak to peak for frequencies higher than 1 Hz with 8 measures taken per decade, and 10 mV peak to peak for frequencies lower than 1 Hz, with 2 integration cycles. The measurement of electrochemical impedance is done alternately with the other electrochemical methods, allowing enough time for the stabilisation of the samples.

The material studied is an API K55 type carbon steel supplied by Valourec Industries (Montbard, France). The average composition by weight per cent of the steel samples is: C: 0.42% (± 0.04); Mn: 1.08% (± 0.001); Mo: 0.014% (± 0.01); Si: 0.34% (± 0.04); Ni: 0.092% (± 0.005); Cr: 0.100% (± 0.005); P: 0.01%; S: 0.004%. The casings of geothermal wells exploiting the Dogger aquifer of the Paris Basin are made of this material.

The corrosive environment is a natural geothermal fluid coming directly from the production wellhead of Melun l'Almont site. This site was chosen because it is also one of the few Dogger sites that have not yet been treated, and because the fluid there is generally representative of the sites to the south of Paris (TDS: 12.7 g/l; surface pH: 6.4; production temperature: 72°C; concentrations (mg/l): $[\text{Na}^+] = 4250$, $[\text{Ca}^{2+}] = 580$, $[\text{Cl}^-] = 7200$, $[\text{SO}_4^{2-}] = 680$, alkalinity $[\text{HCO}_3^-] = 317.0$, $[\text{SiO}_2] = 42.5$; dissolved gas (GLR=14.9%), mainly $\text{CO}_2 = 17.6\%$, $\text{CH}_4 = 53.3\%$, $\text{N}_2 = 19.7\%$. The production flow rate varies over the year between 25 m³/h (in a thermosiphon) and 150 m³/h. The bubble point pressure is around 7 bars. Dissolved sulfide content is 15 mg/l in S^{2-} equivalent.

Depending on the tests to be carried out, we chose one of two types of working electrodes: either cylindrical (diameter of the bar: 7 cm, height: 0.31 cm) with an exposed cylindrical surface area of 2.0 cm², or disk-shaped (diameter: 1.33 cm; thickness: 1.5 mm), with an exposed surface area (flat and circular) of 1.0 cm². Before the experiments the working electrode is polished with sandpaper (320, 600 and 1200 grade), cleaned with acetone or alcohol and deionised water in an ultrasonic bath and then dried in pulsed warm

air. The working electrodes can be stationary or rotating. Concerning the last, it is attached to a turning device (EG&G PARC, RDE 616) whose rotating speed can be varied from 0 to 9,994 rpm. The electrodes are held in place with a metallic rod which is protected against corrosion by a hollow PTFE cylinder.

We chose as a reference a KCl saturated calomel electrode (SCE). At 25°C, the difference in potential with a normal hydrogen electrode (NHE) is 0.2415 V. In tests in geothermal fluid, the electrode potentials are measured in relation to an Ag/AgCl electrode whose potential is 0.223 V/NHE (volts with respect to the NHE electrode). These reference electrodes were connected to the aggressive solutions through a salt bridge. All of the potentials are hereafter reported with respect to the KCl saturated calomel electrode and their unit is given as V/SCE.

In order to minimise the effects of polarisation, we use a large platinum-iridium electrode (Pt 90%, Ir 10%) as a counter electrode. It is made up of a cylindrical grid, 55 mm in diameter and 65 mm high surrounding the working and reference electrodes. Some tests are carried out with a counter electrode built out of the same material but having the shape of a concave plate (2x4 cm²) which does not surround the electrodes but is placed near them.

For the electrochemical studies, the cells are two 500 ml cylindrical "Pyrex" reactors in which the fluid is at atmospheric pressure. Conical holes in its cover permit the attachment of electrodes (temperature, pH and Eh, measurement probes, reference, counter and working electrodes) and the inhibitor injection system.

The electrochemical corrosion techniques were carried out using an EG&G PARC Model 352 system. The impedance measurements were performed using an EG&G PARC Model 398. The set up includes:

- an EG&G PARC potentiostat-galvanostat (model 273A),
- an EG&G PARC lock-in amplifier, model 5210,
- two electrochemical cells
- two HPLC type pumps (SHIMADZU model LC-6A and KNAUER model L64) for the injection of corrosion inhibitor into the two cells
- a BROOKS 8500 flowrate regulator

The piloting of these instruments and the gathering and processing of data are done with a Cheer Personal Computer.

3. RESULTS AND DISCUSSION

Because of the absence of dissolved oxygen in the medium, the half redox reactions are the oxidation of iron into ferrous ions at the anode and the reduction of H^+ ions into H_2 at the cathode.

3.1. Behaviour of the carbon steel at the open circuit potential

Anodic behaviour

The oxidation reaction of iron into ferrous ions is $\text{Fe} \rightarrow \text{Fe}^{2+} + 2\text{e}^-$. The thermodynamic potential of oxidation of iron into ferrous ion, assimilating the activity of Fe^{2+} ions to their concentrations is

$$E_{\text{Fe}^{2+}/\text{Fe}} = E^\circ_{\text{Fe}^{2+}/\text{Fe}} + (RT/2F) \ln [\text{Fe}^{2+}]$$

$E^\circ_{\text{Fe}^{2+}/\text{Fe}} = -0.681 \text{ V/SCE}$ (Besson, 1984), standard potential of the Fe^{2+}/Fe couple.

R is the constant of perfect gases ($R = 8.32 \text{ J K}^{-1} \text{ mol}^{-1}$)

T is the absolute temperature of the electrolyte

F is the Faraday constant ($F = 96450 \text{ C}$)

$[\text{Fe}^{2+}]$ is the concentration of Fe^{2+} ions in solution

At the temperature used in our experiments (65 °C or 338 K), the potential of the anodic reaction of iron dissolution is

$$E_{\text{Fe}^{2+}/\text{Fe}} = -0.681 + 0.03357 \log [\text{Fe}^{2+}]$$

Cathodic behaviour

The reduction of H^+ ions into H_2 is $H^+ + e^- \rightarrow 1/2 H_2$

By assimilating the activity of the H^+ ions to their concentration, the thermodynamic potential of reduction of H^+ ions to the cathode is given by the following equation

$$E_{H^+/H_2} = E^\circ_{H^+/H_2} + RT/F \ln [H^+] - RT/F \ln p_{H_2}^{1/2}$$

Knowing that $E^\circ_{H^+/H_2} = -0.2415$ V/SCE, the thermodynamic reduction potential of H^+ ions at the temperature of the electrolyte (65°C) is:

$$E_{H^+/H_2} = -0.2415 - 0.03357 \log ([H^+]^2/p_{H_2})$$

Open circuit potential, E_{corr}

This is determined by the following equation

$$E_{corr} = E_{H^+/H_2} - E_{Fe^{2+}/Fe}$$

$$E_{corr} = -0.4395 + 0.03357 \log ([H^+]^2/[Fe^{2+}] \cdot p_{H_2})$$

The open circuit potential therefore depends on the Fe^{2+} concentration, the pH and the H_2 partial pressure in the metal/solution interface.

Furthermore, the Fe^{2+} concentration is controlled by the FeS solubility product defined by the equation $K_s(FeS) = [Fe^{2+}][S^{2-}]$

At the anodic sites the Fe^{2+} ions dissolve and later precipitate as FeS when the K_s is reached. The S^{2-} concentration is controlled by the H_2S acidity constants defined by the following equations:

$$K_{a1}(H_2S) = ([HS^-][H^+])/[H_2S] \quad (1)$$

$$K_{a2}(HS^-) = ([S^{2-}][H^+])/[HS^-] \quad (2)$$

If we multiply (1) and (2), we obtain the following relationship:

$$[H^+]^2[S^{2-}]/[H_2S] = K_{a1}(H_2S) \cdot K_{a2}(HS^-), \text{ thus}$$

$$E_{corr} = -0.4395 + 0.03357 \log (K_{a2}HS^- \cdot K_{a1}H_2S \cdot [H_2S])/(K_sFeS \cdot p_{H_2})$$

The E_{corr} depends therefore on the H_2S concentration and the H_2 pressure. Nevertheless, the layer of deposit formed on the surface of the steel contains species such as iron hydroxy-chloride which can influence the redox processes and therefore the corrosion potential

3.2. Behaviour of the carbon steel during linear potential sweep voltammetry in the absence of inhibitor

Anodic behaviour: Anodic polarisation curves clearly show the absence of any passivation domain (Fig 1). This behaviour is justified by the fact that the K55 steel is a soft steel. Furthermore, for both the stationary electrode and the rotating electrode, the anodic polarisation curves show a linear domain beyond +80 mV compared to the corrosion potential. This is characteristic of a pure charge transfer regime. The anodic Tafel slope, ba , slope of the rectilinear part of the anodic polarisation curves, varies depending on the electrode rotating speed. It has an average value of 75 mV/decade at 0 rpm and 60 mV/decade at 1000 rpm after 4 h and 3.5 h of immersion respectively. This difference can be explained by the fact that the iron dissolution kinetics are more rapid in the case of the rotating electrode and are therefore controlled by the electrode rotating speed.

Cathodic behaviour: The cathodic polarisation curves do not show any diffusion plateau (Fig. 1). The reduction reaction is therefore controlled by the charge transfer and is not limited by the input of matter. The cathodic Tafel slope, bc , slope of the linear part of the cathodic polarisation line, varies almost not at all as a function of the electrode rotating speed. It has an average value of 200 mV/decade at 0 rpm and 190 mV/decade at 1000 rpm for a similar immersion time of 4 h and 3.5 hours, respectively. Furthermore, the high bc values compared to ba values show that the reduction reaction is the main control of the corrosion process in the absence of inhibitor.

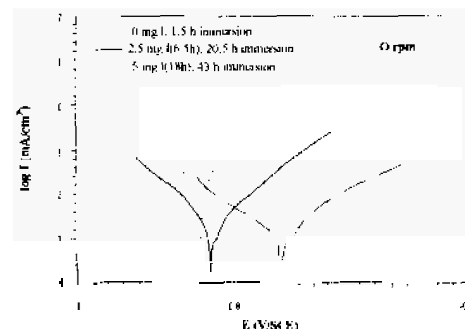


Fig.1 Polarisation curves for carbon steel with different concentrations of Solamine at 0 rpm

Behaviour of carbon steel during the first fifteen hours of immersion without treatment: At 1000 rpm, the corrosion rate decreases rapidly from an initial value of 0.625 to 0.470 mm/y after 3 h of immersion without treatment. It levels out and stabilises at 0.425 mm/y between 6 and 8 h of immersion then decreases rapidly to 0.075 mm/y after 15 h of immersion (Fig 2). At 0 rpm, after an increase of 0.050 mm/y during the first hour of immersion, the corrosion rate decreases rapidly from 0.530 to 0.375 mm/y between the first and the fifth hour of immersion then decreases slowly to 0.300 mm/y after 15 h of immersion. This decrease in the corrosion rate during the first 15 h of immersion might be due to the formation of a protective deposit such as amorphous iron sulfide whose relatively dense structure and low porosity would contribute to ensure a better protection of the metal. Moreover, during the first fifteen hours of immersion, the open circuit potential of both samples is relatively stable at -830 mV/SCE and -815 mV/SCE for the stationary and rotating samples, respectively. In the case of the rotating electrode, the shift of the corrosion potential towards more noble potentials can be explained by an increase in the kinetics of the reduction reaction occurring at the surface of the scale. Indeed, the hydrodynamic regime created by the rotating electrode might contribute to the formation of a layer of iron sulfide more homogeneous than in the case of a stationary electrode, facilitating the discharge of the hydrogen. This phenomenon could explain the higher corrosion rates observed in the case of the rotating electrode during the first 10 h of immersion.

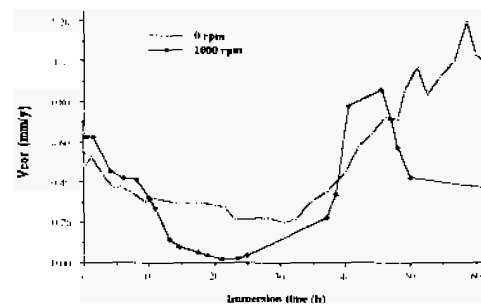


Fig. 2. Corrosion rate as a function of the electrode rotating speed during the first sixty five hours of immersion without treatment

Behaviour of carbon steel between fifteen and sixty-five hours of immersion without treatment: At 1000 rpm, the corrosion rate of steel between 22 and 45 h of immersion increases 12-fold, evolving very rapidly from 0.070 to 0.85 mm/y (Fig 2). The corrosion rate of the stationary sample also rises sharply from 0.2 to 1.2 mm/y between 30 and 70 h of immersion (Fig 2). This phenomenon can be explained by a crystallisation of the amorphous iron sulfide which causes an increase in the porosity of the scale and therefore an increase in the corrosion rate. Moreover, this crystallisation seems to be kinetically activated by the electrode rotating speed. Indeed, the moderate decrease in the corrosion rate at 1000 rpm after 45 h of immersion (Fig 2) is probably due to the fact that the crystals formed are larger and more protective. This is also corroborated by the fact that at 0 rpm the increase in the corrosion rate after 30 h of immersion is progressive and a sign of slow crystallisation kinetics. The deposition

of a great quantity of amorphous FeS after the high corrosion rate can also explain this decrease in corrosion rate.

3.3. Behaviour of carbon steel when corrosion inhibitors are added

Addition of 2.5 mg/l after the first phase of immersion without treatment

The effectiveness of the various inhibitors was evaluated over a period of 10 h of treatment with 2.5 mg/l of inhibitor after a first phase of immersion without treatment. This enabled us to evaluate the action of the inhibitors in the presence of scale and simulate real conditions encountered in geothermal doublets which have been operating for several years.

Stationary sample

After adding 2.5 mg/l, the six inhibitors decrease significantly the corrosion rate, notably butyric Amine and Soluble Amine for which the effectiveness is, respectively, 87.5 and 92% after two hours of treatment (Table 1). Aquaprox and Solamine are 79 and 64.5% effective for similar treatment and immersion times. These differences in corrosion rate two hours after the beginning of treatment are caused by different adsorption kinetics, the most rapid being those of Soluble Amine and Fatty Amine. Norust and Cyclic Amine, on the other hand, have much slower adsorption kinetics. Their effectiveness after two hours of treatment is only 46.9 and 25%, respectively. Ten hours after the start of treatment, the difference between inhibitors is less marked. They are all nearly or more than 90% effective except Norust which is only 23.6% effective, a value lower than its effectiveness after two hours of treatment (Table 1).

In presence of the six inhibitors the open circuit potential becomes more noble during treatment with 2.5 mg/l of inhibitor. This shift of potential ranges from +45 mV (for Norust) to +112 mV (for Soluble Amine) after 10 h of treatment (Table 1).

The analysis of the impedance diagram shows the absence of coating action of the inhibitors during this first phase of treatment with 2.5 mg/l of inhibitor for around 10 h. The electrochemical impedance measurements revealed the effect of inhibitor on the decrease in the corrosion rate. Indeed, in all cases, the addition of 2.5 mg/l of inhibitor caused a decrease in the capacity of the double layer and an increase in the diameter of the capacitive loop. This diameter is simply the polarisation resistance identical to that determined by polarising the sample at ± 20 mV on either side of E_{corr} . The results of the two methods are similar. Therefore, for Cyclic Amine, the polarisation resistance method gives R_p values of 218 and 340 $\Omega \cdot \text{cm}^2$, respectively, at 0 and 2.5 mg/l (15 h of treatment) while electrochemical impedance gives values of 206 and 320 $\Omega \cdot \text{cm}^2$ for the same immersion time and treatment conditions (Fig. 3).

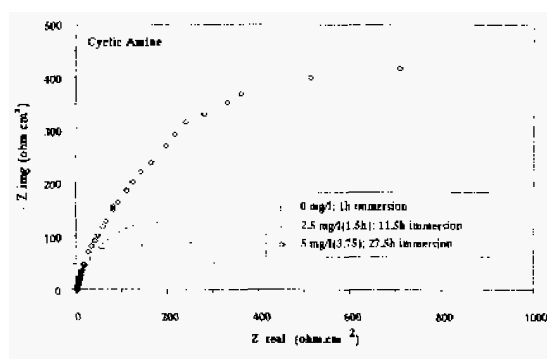


Fig. 3 Electrochemical impedance diagram for a stationary sample as a function of time and Cyclic Amine concentration at 0 rpm

Fatty Amine and Soluble Amine increase E_{oc} and decrease i_{corr} and reduce the corrosion current while shifting the corrosion potential

towards cathodic values. They act as mixed inhibitors. Solamine, which does not modify E_{oc} and decreases i_{corr} is a cathodic inhibitor, causing a shift in the corrosion potential towards more noble values (Fig. 1). The three other inhibitors, which cause a decrease in i_{corr} and E_{oc} make the potential more noble but, like Solamine, their action decreases two hours after their injection because their adsorption kinetics at anodic sites seems to be slower. The inhibiting effect of Norust at 2.5 mg/l is less than 50% and does not increase with the length of treatment.

Rotating sample

Corrosion tests run on rotating samples (1000 rpm) are compared to stationary tests under the same treatment and immersion time conditions—2.5 mg/l of inhibitor added for 10 h after an immersion phase of 10 to 15 h without treatment.

The decrease in the corrosion rate is very significant right from the start of treatment. The corrosion rate is indeed lower than 0.067 mm/y after two hours of treatment for all the inhibitors except Fatty Amine and Solamine. On the average, the inhibitors are 89% effective after two hours of treatment, except for Aquaprox which is only 44% effective (Table 1). This behaviour during the first hours after injection is different from what was observed in the case of the stationary electrode and shows the influence of the hydrodynamic regime created by the rotating electrode on the adsorption kinetics of inhibitors.

Thus, for Cyclic Amine and Norust, passing from 0 to 1000 rpm increases the effectiveness 4-fold and 2-fold, respectively. The increase in i_{corr} observed when we pass from 0 to 1000 rpm suggests that the increased effectiveness of these two inhibitors at 1000 rpm is due to an activation of the adsorption kinetics at the anodic sites.

The effectiveness of Soluble Amine after 10 h of treatment is half what it had been after two hours of treatment. Aquaprox and Cyclic Amine behave in a similar manner, although with a more moderate decrease of around 30% in their inhibiting effectiveness. The inhibiting power of Fatty Amine, which was ineffective after two hours of treatment, increases with the length of treatment. This is not the case for Solamine which remains ineffective after two hours of treatment. Norust was very effective, its level of inhibition remained at around 80% (Table 1).

As for the stationary sample, the six inhibitors make the metal more noble, the greatest effect being that of Solamine (+265 mV). Fatty Amine shifts the potential only by -90 mV and the four other inhibitors by an average of -230 mV (Table 1). The increase in corrosion potential is therefore clearly marked for the rotating sample. The average shift caused by the inhibitors is +210 mV, while it was around +72 mV for stationary samples.

The electrochemical impedance diagrams obtained for the rotating electrode are similar to those of the stationary sample. Nevertheless, the values for polarisation resistance at 1000 rpm are higher. Therefore, for Cyclic Amine, the polarisation resistance is 4276 $\Omega \cdot \text{cm}^2$ after almost 4 h of treatment with 2.5 mg/l at 1000 rpm while it is 320 $\Omega \cdot \text{cm}^2$ after 15 h of treatment with 2.5 mg/l at 0 rpm. This is in agreement with observations mentioned above.

In the case of the rotating electrode, all of the inhibitors increase the anodic Tafel slope and decrease the cathodic Tafel slope. They are mixed inhibitors (anodic and cathodic) which make the metal more noble. Cyclic Amine, Norust, Soluble Amine adsorb most rapidly. Aquaprox has a low adsorption rate which even diminishes with time. The effectiveness of Solamine and Fatty Amine is mediocre or even nil under such conditions of immersion and hydrodynamic regime. Electrochemical impedance measurements did not reveal any coating action with 2.5 mg/l and for around 10 h of treatment.

The effect of adding an additional 2.5 mg/l of inhibitor after the initial treatment with 2.5 mg/l

The effect of adding 5 mg/l of inhibitor was studied for around 10 hours after the end of the first phase of treatment with 2.5 mg/l of inhibitor.

Stationary sample

The evolution of the corrosion rate when the quantity was increased from 2.5 to 5 mg/l varied depending on the nature of the inhibitor. The adding of 5 mg/l increases the effectiveness of Norust 4-fold (Table 1). For Fatty Amine, Aquaprox and Solamine, the adding of an additional 2.5 mg/l has no effect. Nevertheless, the increase in the diameter of the capacitive loop (in the impedance diagrams) resulting from the addition of 2.5 mg/l attests to the increase in effectiveness of the inhibitor at this concentration (Fig 3).

3.5. The effect of stopping treatment

While there was no increase in the corrosion rate 6 h after treatment with 5 mg/l of Solamine was stopped. 16 hours after treatment was stopped the effectiveness of Solamine was only 68%, down from 98% when treatment was stopped. This means that 30% of the inhibitor had been desorbed. With Cyclic Amine, 6 h after treatment was stopped, the corrosion rate was unchanged but was twice as great 16 hours after treatment had stopped. Soluble Amine does not desorb 8 h after the end of treatment because no variation in the corrosion

Table 1. Comparison of the effectiveness (E_{inh}) and corrosion potential (E_{corr}) Variation for the different inhibitors with various concentrations and immersion times (T_{imm}) at 0 and 1000 rpm. NM: Not measured or not measurable.

		without treatment	2 hours of treatment with 2.5 mg/l					without treatment	10 hours of treatment with 5 mg/l					without treatment	10 hours of treatment with 2.5 mg/l		
Name of inhibitor	T_{rms}	V_{corr}	V_{corr}	E_{inh}	T_{rms}	V_{corr}	V_{corr}	E_{inh}	E_{corr}	variation	T_{rms}	V_{corr}	V_{corr}	E_{inh}	E_{corr}	variation	
	h	mm/y	mm/y	%	h	mm/y	mm/y	%	mV		h	mm/y	mm/y	%	mV		
at 0rpm																	
Fatty Amine	12.00	0.32	0.04	87.5	20	0.275	0.015	94.5	60	30.00	0.24	0.026	89.2	60			
Soluble Amine	15.00	0.31	0.025	92.0	23	0.21	0.015	92.9	112	NM	NM	NM	NM	NM			
Aquaprox	17.25	0.31	0.065	79.0	25.25	0.21	0.02	90.5	53	35.5	0.308	0.038	87.7	111			
Solamine	16.00	0.31	0.11	64.5	24	0.21	0.016	92	69	34.00	0.438	0.02	95.4	34			
Norust	11.5	0.32	0.17	46.9	19.5	0.275	0.21	23.6	45	39.5	0.185	0.013	93	95			
Cyclic Amine	12.00	0.32	0.24	25.0	20	0.275	0.03	89	92	30.00	NM	NM	NM	30			
at 1000 rpm																	
Fatty Amine	10.75	0.175	0.19	NM	18.75	0.03	0.02	33.3	90	32.00	0.143	0.008	94.4	37.5			
Soluble Amine	9.00	0.36	0.04	88.9	17	0.05	0.03	40.0	240	28.00	0.085	0.038	55.3	112.5			
Aquaprox	12.00	0.12	0.067	44.2	20	0.03	0.02	33.3	230	31.00	0.125	0.02	84.0	47			
Solamine	17.75	0.05	0.1	NM	25.75	0.065	0.1	NM	265	41.00	0.5	0.038	92.4	62.5			
Norust	8.00	0.4	0.065	83.8	16	0.063	0.012	81.0	230	NM	NM	NM	NM	NM			
Cyclic Amine	6.00	0.42	0.025	94.0	14	0.08	0.025	68.8	205	46.00	NM	0.022	NM	45			

Rotating sample

Increasing the inhibitor to 5 mg/l increases the effectiveness of Fatty Amine 3-fold and that of Aquaprox 2.5-fold (Table 1). There is a spectacular rise in the effectiveness with Solamine and a more moderate increase with Soluble Amine for which the effectiveness is only 55% after 28 h of treatment. It therefore seems that Soluble Amine has a restrained action on the inhibition of iron sulfide crystal growth for which we have hypothesised a crystallisation after 22 h of immersion at 1000 rpm (see paragraph 3.2).

3.1. The effect of immersion time on the effectiveness of the inhibitor

We compared the behaviour of inhibitors at immersion times for which there was an increase in the corrosion rate between 22 and 45 hours for the rotating sample and between 30 and 70 hours for the stationary sample (see paragraph 3.2.). Nevertheless, because of the lack of data beyond 35 hours of immersion without treatment at 1000 rpm we had to limit our study to the behaviour at 0 rpm. For Soluble Amine at 0 rpm, we noted a decrease in effectiveness with 2.5 mg/l after 30 hours of immersion. Therefore, at 20 hours of immersion and compared with the case without treatment, it reduces the corrosion rate from 0.27 to 0.015 mm/y, in other words an effectiveness of 94% while at 40 hours of immersion its effectiveness is only 71% (Fig 4). For Aquaprox, no decrease in effectiveness was observed. Indeed, after 30 hours of immersion, this inhibitor is 87.5% effective while it is 87.9% effective after 40 hours.

No increase in the corrosion rate is measured after 30 hours of immersion at 0 rpm for Solamine and Norust. Likewise, the effectiveness of Cyclic Amine passes from 11 to 88% at similar immersion times. These four inhibitors therefore have a very positive behaviour concerning the inhibition of crystal growth. On the other hand, Fatty Amine shows a slight decrease in effectiveness from 92.5 to 82.2% between 30 and 44 hours of immersion. These results confirm the effectiveness of 2.5 mg/l of Soluble Amine in the presence of crystallised iron sulfide and show that Cyclic Amine, Solamine, Aquaprox and Norust have a good behaviour at 2.5 mg/l in the presence of crystal growth of scale. The inhibiting action of Fatty Amine is slightly affected by the presence of crystallised deposits.

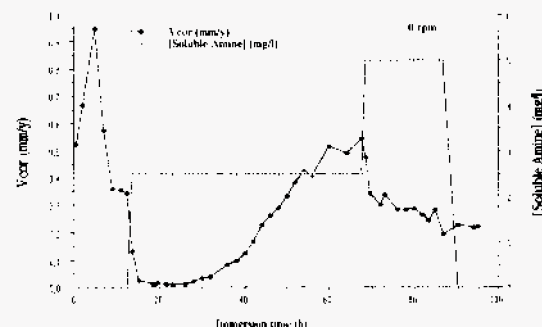


Fig. 4. Corrosion rate as a function of Soluble Amine concentration and immersion time at 0 rpm

rate is observed. The effectiveness of Fatty Amine decreased from 87% when treatment was stopped to 84% 5 hours later proving that this inhibitor is almost not desorbed. On the other hand, 10 hours after the end of treatment, the effectiveness is only 46%, or about 40% of the inhibitor is desorbed. We have no data concerning the effectiveness of Aquaprox and Norust after the stopping of treatment.

4. CONCLUSION

Work carried out on site enabled us to study the effect of real geothermal fluid and the adding of various inhibitors on the corrosion of carbon steel. We were able to ensure a constant fluid temperature, pressure and physico-chemistry during the total duration of the tests.

In the real fluid, as in the partially reconstituted fluid, scale plays a preponderant role in the evolution of the corrosion, especially in the case of the real fluid, where the study of the cathodic slopes of the Tafel lines, shows that the cathodic reaction probably occurs entirely on the scale and controls the kinetics of the corrosion reactions. Without treatment, the large decrease in the corrosion rate of steel which was seen during the first 20 hours of immersion is due to the formation of amorphous iron sulfide which temporarily protects the metal.

In the case of the rotating electrode, it was also shown that the hydrodynamic regime thus created has a direct influence on the homogeneity of the scale. Indeed, the rotation of the electrode ensures a better distribution of the iron sulfide, facilitating the discharge of the hydrogen. This phenomenon explains the higher corrosion rates observed at 1000 rpm during the first hours of immersion. Amorphous iron sulfide crystallisation was also shown after 22 and 30 hours of immersion at 1000 and 0 rpm, respectively. For these immersion times, we noted a large rise in the corrosion rate, the kinetics of which would be controlled by the electrode rotating speed. Analyses of scale sampled at various periods of immersion will be used to study these phenomena.

At 0 rpm, the injection of 2.5 mg/l of inhibitor after a phase of immersion without treatment of 10 to 15 hours showed very rapid adsorption kinetics for Fatty Amine and Soluble Amine for which the inhibition rate was around 90% two hours after injection. While the effect of Aquaprox, Solamine and Cyclic Amine on the decrease of the corrosion rate right from the onset of treatment is less evident, they are nevertheless 90% effective after 10 hours of treatment. On the other hand, Norust has the slowest adsorption kinetics with a mediocre inhibition rate which does not increase with the length of treatment. The injection of 5 mg/l does not significantly increase the effectiveness of the inhibitors except in the case of Norust for which it increases 4-fold after 10 hours of treatment.

The differences seen in the action of inhibitors on the evolution of anodic and cathodic Tafel slopes between the stationary and rotating electrode clearly show that the behaviour of the inhibitor on the redox reaction kinetics is controlled by the electrode rotating speed. As a result, there are large differences in the inhibition action. The effectiveness of Norust increases 2-fold when we pass from 0 to 1000 rpm for similar treatment and immersion time. On the other hand, the inhibiting action of Solamine, Fatty Amine and Aquaprox is considerably reduced at 1000 rpm.

At 0 rpm, an increase in the immersion time also caused a significant decrease in the effectiveness of Soluble Amine injected at 2.5 mg/l in the presence of crystalline iron sulfide scale. On the other hand, Cyclic Amine, Solamine, Aquaprox and Norust seem to effectively inhibit crystal growth. The effectiveness of Fatty Amine is slightly affected by the presence of crystallised scale.

The stopping of treatment revealed relatively similar desorption kinetics for Solamine, Cyclic Amine, Soluble Amine and Fatty Amine. On the average, 6 hours after the end of treatment, no increase in the corrosion rate was observed. The desorption rate of Fatty Amine seems slower though because the corrosion rate 8 hours after the end of the injection is identical to what was observed at the onset of the end of treatment.

The 6 inhibitors tested all seem to decrease the value of the cathodic Tafel slope, decreasing the cathodic overpotential and limiting the process of reduction and therefore of corrosion. They seem to act by blocking the cathodic sites thus causing an inhibition of the discharge of hydrogen at the iron sulfide. On the other hand, their action on the oxidation reaction is controlled by the electrode rotating speed the effect of which seems preponderant on the behaviour of the inhibitor at the anodic sites.

The results of the analysis of impedance diagrams are concordant with those of polarisation methods. The electrochemical impedance curves on the Nyquist plane show that corrosion under these conditions is controlled by the charge transfer. The diagrams show only one capacitive loop whose diameter is the same as the polarisation resistance calculated using polarisation techniques. This also shows that the scale formed does not form a physical barrier to the mass transfer between the solution and the metal, capable of modifying the global corrosion kinetics. The coating action of the

inhibitors was not observed at concentrations of 2.5 and 5 mg/l under conditions of immersion time and length of treatment of our experiments.

ACKNOWLEDGMENTS: This is the BRGM contribution.

N°95006. This work was carried out in the framework of the Commission of European Communities contract N°JOU2-CT92-0108, and received financial support from a BRGM research project (S08).

REFERENCES

- Amalhay M., Gauthier B., Ignatiadis I. (1994a) - The influence of some physico-chemical parameters and exploitation conditions on corrosion and scaling in geothermal wells in the Paris Basin. In: *Proceedings of the International Symposium, Geothermics 94 in Europe, from Research to Development*, BRGM (ed), Orléans, France, 8-9 February 1994, pp. 233-240.
- Amalhay M., Abou Akar A., Ignatiadis I. (1994b) - Study of scale deposition phenomena in geothermal wells in the Paris Basin. In: *Proceedings of the International Symposium, Geothermics 94 in Europe, from Research to Development*, BRGM (ed), Orléans, France, 8-9 February 1994, pp. 223-232.
- Besson J. (1984) *Précis de thermodynamique et cinétique électrochimiques*, Ellipses - Edition Mark, Paris, 160pp.
- Crolet J.L. (1988) Mécanismes de la corrosion uniforme sous dépôt de corrosion, *Métaux Corrosion Industries*, Vol LXIII, n°757, pp 279-302.
- Ellis P.E. (1981) A geothermal corrosivity classification system. *Geothermal Resources Council, IRANSACKIONS*, Vol 5, pp 463-466.
- Ikeda A., Ueda M., Mukai S. (1985a) - Proc. Inter Corr Forum Corrosion 85 at Boston, NACE, paper n° 29.
- Ikeda A., Mukai S., Ueda M. (1985b) CO₂ corrosion behavior of carbon and Cr steel. *The Sumitomo Search* Vol 31, p 91-102.
- Lin L.F., Chao C., Macdonald D.D. (1981) - *J. electrochem Soc.*, Vol 128, 6, pp.1194.
- Lin L.F., Chao C., Macdonald D.D. (1984) - 5e Symposium international sur la passivité (Bombarne), 30 mai-3 juin 1984.
- Pickering H.W., Frankenthal R. (1972) - *J. Electrochem Soc.*, Vol 119, n°10, p 1297.
- Pou T.E., Murphy O.J., Young V., Bochrus J.O.M. (1984) - 8e Congrès international de corrosion métallique, Toronto, 3-7 juin 1984.
- Pound B.G., Wright G.A., Sharp R.M. (1980) Geothermal corrosion, in *Chemistry in New Zealand*, pp 183-186.
- Pound B.G., Abdurrahman M.H., Glucina P., Wright G.A., Sharp R.M. (1985) The corrosion of carbon steel and stainless steel in simulated geothermal media. *Aust J. Chem.*, Vol 38, p 1133-1140.
- Sato N. (1982) - *J. Electrochem Soc.*, Vol 129, n° 2, pp 255-260.
- Stem M., Geary A.L. (1957) *J. Electrochem Soc.*, Vol 104, n°9, pp 559-564.